Reversible room-temperature ferromagnetism in Nb-doped SrTiO₃ single crystals

Z. Q. Liu,[1,2] W. M. Lü,[1,3] S. L. Lim,[2] X. P. Qiu,[3] N. N. Bao,[1] M. Motapothula,[1,4] J. B. Yi,[5] M. Yang,[2] S. Dhar,[1,3] T. Venkatesan,[1,2,3] and Ariando[1,2,*]

[1]*NUSNNI-Nanocore, National University of Singapore, 117411 Singapore*

[2]*Department of Physics, National University of Singapore, 117542 Singapore*

[3]*Department of Electrical and Computer Engineering, National University of Singapore, 117576 Singapore*

[4]*Center for Ion Beam Applications, National University of Singapore, 117542 Singapore*

[5]*Department of Material Science and Engineering, National University of Singapore, 117576 Singapore*

The search for oxide-based room-temperature ferromagnetism has been one of the holy grails in condensed matter physics. Room-temperature ferromagnetism observed in Nb-doped SrTiO₃ single crystals is reported in this Rapid Communication. The ferromagnetism can be eliminated by air annealing (making the samples predominantly diamagnetic) and can be recovered by subsequent vacuum annealing. The temperature dependence of magnetic moment resembles the temperature dependence of carrier density, indicating that the magnetism is closely related to the free carriers. Our results suggest that the ferromagnetism is induced by oxygen vacancies. In addition, hysteretic magnetoresistance was observed for magnetic field parallel to the current, indicating that the magnetic moments are in the plane of the samples. The x-ray photoemission spectroscopy, the static time-of-flight and the dynamic secondary ion mass spectroscopy and proton induced x-ray emission measurements were performed to examine the magnetic impurities, showing that the observed ferromagnetism is unlikely due to any magnetic contaminant.

PACS number(s): 75.47.Lx, 75.50.Pp, 75.70.Rf

The potential for discovering new magnetic interactions with possible applications in spintronic devices has been the main driver for the search of oxide-based room-temperature ferromagnetism (RTFM).[1,2] Since the theoretical prediction of RTFM in Mn-doped ZnO (see Ref. 3) and the experimental observation of RTFM in Co-doped TiO₂ (see Ref. 4), dilute magnetic semiconductors (DMS) have attracted significant attention from the community of oxide electronics. Typically, DMS are fabricated by introducing magnetic ions into wide band-gap semiconductors including ZnO, TiO₂, SnO₂,[5] and In₂O₃.[6] In addition, since the finding of unexpected ferromagnetism in insulating HfO₂ thin films[7] in 2004, RTFM was also observed in pristine TiO₂,[8,9] In₂O₃,[9] ZnO,[10,11] and SnO₂[12] thin films without magnetic dopants. All of these results were attributed to oxygen vacancies or other ionic defects.

SrTiO₃ (STO) is important for oxide electronics due to its chemical and thermal stabilities, as well as the lattice match to a large number of functional perovskite materials. Pristine STO is a typical nonpolar band insulator with an indirect band gap of 3.25 eV and a direct band gap of 3.75 eV.[13] However, the slight doping of Nb can shift the Fermi level of STO up or even into the bottom of its conduction band, thus giving an *n*-type semiconducting or metallic phase.[14] Nb-doped SrTiO₃ (NSTO) is a low-temperature two-band superconductor,[15] with strong interactions among electrons, plasmons, phonons, and polarons.[16,17] More importantly, it is one of the most used substrates for oxide film deposition and oxide electronic device applications.[18]

A pristine STO single crystal is an ideal diamagnet due to the absence of unpaired electrons. The Nb doping replaces some of Ti atoms and the resultant Ti³⁺ ions with unpaired electrons can generate a basic paramagnetic response to an external magnetic field. Here, we report RTFM observed in NSTO single-crystal substrates, which is found to be induced

by oxygen vacancies and possibly mediated by free electrons from Nb doping. We examined the transport and magnetic properties of 5 mm × 5 mm × 0.5 mm NSTO single crystals with different dopings, i.e., 0.05, 0.1, 0.5 (CrysTec GmbH, Germany), 0.7 (Hefei Kejing Material Technology Co., Ltd., China), and 1 wt% (MTI, USA). The transport and magnetic properties were measured in a Quantum Design PPMS and a Quantum Design SQUID-VSM tool, respectively.

The temperature dependencies of resistivity from 300 to 2 K for different NSTO single crystals are shown on a logarithmic scale in Fig. 1. All of them show typical metallic behavior and the resistivity of NSTO decreases with the doping level over the whole temperature range. The moment versus temperature (*M-T*) measurements were performed for NSTO single crystals by a 1000 Oe magnetic field applied parallel to the surface of samples. The *M-T* curves of NSTO single crystals are shown in Fig. 2. For 0.05 and 0.1 wt% dopings, negative magnetic moment over the whole temperature range in Fig. 2(a) indicates that the diamagnetism from STO matrix is dominant. The magnetic moment versus magnetic field (*M-H*) curves measured up to 2000 Oe show linear field dependence of moment even at low temperatures down to 2 K as seen in the inset of Fig. 2(a). These demonstrate that only diamagnetism and paramagnetism coexist in 0.05 wt% and 0.1 wt% NSTO single crystals, and paramagnetism leads to a slight increase of magnetic moment at low temperatures.

The *M-T* curve of a 0.5 wt% NSTO single crystal is shown in Fig. 2(b), which is evidently distinct from the *M-T* curves for single crystals with lighter doping. Unexpectedly, the magnetic moment peaks at around 60 K and ferromagnetic hysteresis loops can be seen from 2 to 300 K as shown in Fig. 2(c). The average coercivity field is between 300 and 400 Oe. The saturation ferromagnetic moment at 2 K is 5 × 10⁻⁶ emu and the corresponding magnetization for the whole
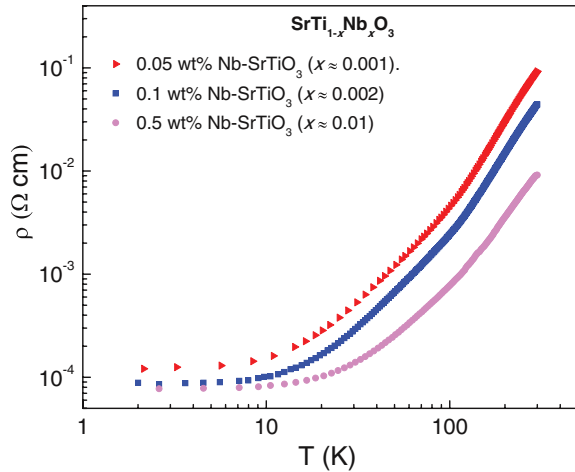
FIG. 1. (Color online) Temperature dependence of resistivity of Nb-doped $SrTiO_3$ (NSTO) single crystals with different dopings.

5 mm $\times$ 5 mm $\times$ 0.5 mm single crystal is 4×10^{-4} emu/cm^3, which is equivalent to 5×10^{-3} Oe. The average ferromagnetic moment for each Nb atom (or roughly each free electron) of NSTO is $2.65 \times 10^{-4} \mu_B$, which is two orders of magnitude smaller than the ferromagnetic moment of free-electron gas, $0.07 \mu_B$/electron reported by Young *et al.*[19]

NSTO single crystals from different batches and different vendors were investigated. It was found that all of 0.5 wt% samples (CrysTec GmbH, Germany) show ferromagnetic hysteresis loop with the same order of magnitude of the magnetic moment at 2 K as well as 300 K.[20] Moreover, the 0.7 wt% NSTO single crystal (from Hefei Kejing Material Technology Co., Ltd., China) and 1 wt% NSTO (from MTI, USA) also show similar ferromagnetic hysteresis loops at both 2 and 300 K.[20] Assuming that the ferromagnetism originates from some ferromagnetic artifacts, like Fe, which can maximally supply 2.2 μ_B/atom to ferromagnetism, the
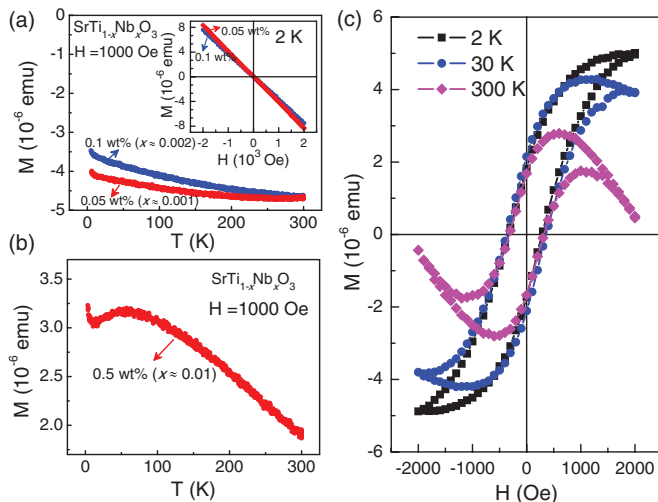
FIG. 2. (Color online) Magnetic moment of 5 mm $\times$ 5 mm $\times$ 0.5 mm NSTO. (a) Magnetic moment vs temperature (*M-T*) curves of 0.05 wt% and 0.1 wt% NSTO. (Inset) *M-H* curves at 2 K. (b) *M-T* curve of 0.5 wt% NSTO. (c) Magnetic moment vs magnetic field (*M-H*) curves of 0.5 wt% NSTO at 2, 30, and 300 K.
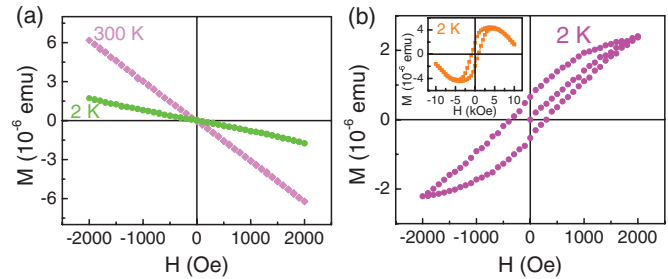
FIG. 3. (Color online) Magnetic moment of 0.5 wt% NSTO for continuous annealing procedures. (a) *M-H* curves at 2 and 300 K after annealing at 600 °C in air for 2 h. (b) *M-H* curves at 2 K upon the subsequent vacuum annealing at 950 °C in $\sim 10^{-7}$ Torr vacuum for 1 h. (Inset) *M-H* loop at 2 K measured up to 1 T.

corresponding minimum density of Fe impurity of $\sim 1.96 \times 10^{16}$ atoms/cm^3 is required in 0.5 wt% NSTO. It is within the typical detection limit of static time-of-flight secondary ion mass spectroscopy (SIMS).[21] SIMS analysis of possible Fe, Co, Ni, Cr, Mn, and Cu elements were performed down to more than 400 nm below the surface at different regions of the sample but no trace of them was observed.[20] In addition, x-ray photoemission spectroscopy (XPS) examination with Ar ion milling was carried out down to more than 100 nm below the surface. The wavelength regions of the characteristic photoemission peaks of possible Fe, Co, and Ni elements were carefully examined but also no signature of them was seen.[20]

Later, it was found that the ferromagnetism can greatly decrease or even disappear after annealing single crystals in air. The *M-H* hysteresis at 2 and 300 K completely disappear after annealing at 600 °C for 2 h, as shown in Fig. 3(a). Subsequently, the sample was vacuum-annealed at 950 °C in $\sim 10^{-7}$ Torr vacuum for 1 h and the ferromagnetism was recovered [see Fig. 3(b)]. Upon fitting and subtraction of the diamagnetic signal, the pure ferromagnetic loop can be extracted from the *M-H* loop up to 1 T.[20] The final saturation ferromagnetic moment recovered from vacuum annealing is $\sim 8.5 \times 10^{-6}$ emu, which is of the same order of magnitude with the ferromagnetic signal in the original case. These results indicate that the ferromagnetism is closely related to oxygen vacancies in NSTO single crystals. Moreover, it was found that the ferromagnetic moment in an as-received 0.5 wt% NSTO single crystal significantly decreases even after annealing in air at 250 °C for 30 mins.[20] As the diffusion coefficient D of oxygen ion in STO below 450 °C is less than 10^{-16} cm^2/s (see Ref. [22]), the diffusion length $l = \sqrt{Dt}$ is therefore less than 40 nm for 30 mins. This indicates that the ferromagnetic moments mostly exist in the surface region of NSTO single crystals.

To further examine possible impurities of Cr, Mn, Fe, Co, Ni, and Cu in vacuum-annealed samples, we performed dynamic SIMS measurements using a Cameca IMS-6f magnetic sector spectrometer with a sensitivity of parts per billion (ppb), which is three orders of magnitude higher than the sensitivity of the typical static time-of-flight SIMS. During the analysis, a Cs$^+$ primary ion beam of 10 keV was rastered over an area of $250 \times 250 \, \mu$m^2, with the samples biased at a voltage of +5 kV. Positive secondary ions were acquired from a central area of approximately 40 μm in diameter. Depth profiling spectra were first acquired over a thickness of approximately 500 nm,
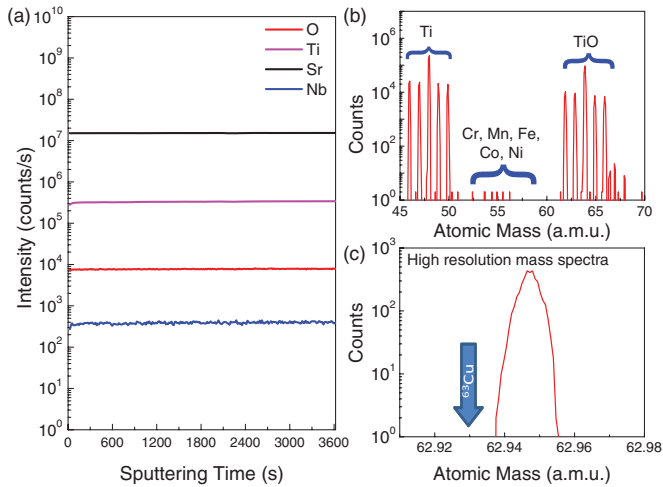
FIG. 4. (Color online) Dynamic SIMS. (a) Depth profiling spectra of a vacuum-annealed 0.5 wt% NSTO single crystal. (b) Mass spectra over the mass range of 45–70 amu. (c) High-resolution mass spectra at the mass range of $^{47}Ti^{16}O$.

within which the matrix elements were observed to be uniform as shown for a vacuum-annealed sample in Fig. 4(a). At the specified depth, mass spectra were then collected over the mass range of interest (45–70 amu), which confirmed the absence of Cr, Mn, Fe, Co, and Ni impurities [see Fig. 4(b)]. Due to the mass interference of ^{63}Cu with $^{47}Ti^{16}O$, high resolution mass spectra were acquired at the mass range of $^{47}Ti^{16}O$ (with mass resolution higher than 5000). No signal of ^{63}Cu was detected as indicated by the arrow in Fig. 4(c). Since the SIMS experiment only probes the surface of the samples (around 500 nm in depth), we performed proton induced x-ray emission experiments (PIXE) where the 2.1 MeV proton beam is able to probe a depth of 60 μm. The dominant impurities were found to be Fe and Zn at 2.1 and 0.4 at%, respectively, for the oxygen annealed samples (diamagnetic), while for vacuum annealed samples (ferromagnetic) the concentrations were 1.5 and 1.3 at%, respectively. Clearly, these impurities are highly mobile during the various annealing processing steps, but they do not show any correlation with respect to the observed magnetic properties. This implies that the surface region must be the sole contributor to the observed ferromagnetism. The variation of the impurities in the deeper layer does not affect the observed magnetism. This is consistent with the experiment where 2 at% magnetic elements (Fe, Cr, Co and Mn) were intentionally added to epitaxial NSTO films but no ferromagnetism was seen.[23]

The magnetoresistance (MR) of 0.5 wt% NSTO single crystals was studied. Transverse MR is positive and quadratically depends on magnetic field,[20] which suggests that the orbital scattering dominates due to the Lorentz force. No hysteresis in transverse MR curves was observed. Nevertheless, as the magnetic field is applied parallel to the current, negative MR shows up. More importantly, there is a hysteresis loop in the MR curve (see Fig. 5), typical of ferromagnetic materials.[24] Nevertheless, the MR loop here exhibits double peaks in a single round field scan from −9 to 9 T or 9 to −9 T, which is different from that of conventional ferromagnetic materials.[24] The double peaks could be that STO is a
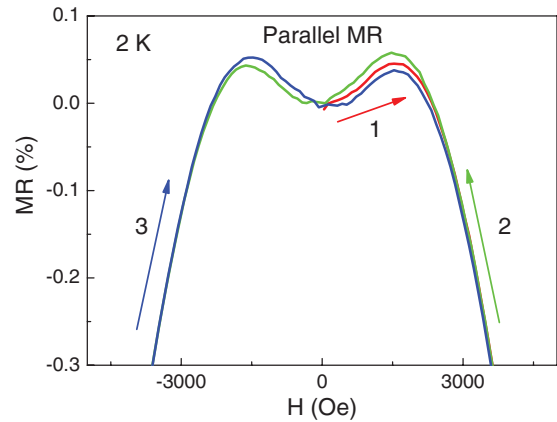
FIG. 5. (Color online) Parallel MR of a 0.5 wt% NSTO single crystal at 2 K. The numbers 1, 2, and 3 indicate the measurement sequence.

high-mobility system and accordingly positive MR from orbital scattering could dominate at low field if the current is not well-confined to be exactly parallel to magnetic field, which are commonly observed in STO-based electron systems.[25–28] Moreover, the saturation field in the ferromagnetic hysteresis loop is consistent with the closure field in the MR data. The hysteresis reveals that the ferromagnetism observed in NSTO single crystals is intrinsic.

The temperature dependence of carrier density (n-T) for as-received NSTO single crystals were measured via Van der Pauw Hall geometry with two voltage and two current electrodes placed at the four corners of 5 mm × 5 mm square single crystals. No anomalous Hall effect was obtained, which is likely because the ferromagnetic moment mostly existing in the surface region is too small for an entire single crystal to generate the anomalous Hall effect. Intriguingly, it was found that the carrier density of NSTO first increases with lowering temperature, and then peaks at a certain temperature resembling its M-T curve, as shown in Fig. 6(a). The structural phase
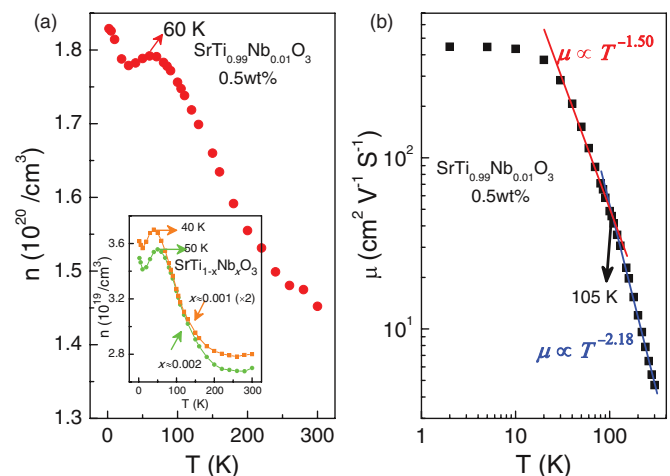
FIG. 6. (Color online) (a) Temperature dependence of carrier density (n-T) of NSTO single crystals. (Inset) n-T curves of 0.05 and 0.1 wt% NSTO. For clarity, the carrier density of the 0.05 wt% NSTO sample is multiplied by a factor of two. (b) Temperature dependence of mobility (μ) of the 0.5 wt% NSTO single crystal.

transition of bulk STO at ∼105 K can be clearly seen from the linear power law fittings of the temperature dependence of mobility in Fig. 6(b), which was also observed in oxygen-deficient STO single crystals.[29] The peak temperature depends on the doping level. For 0.5 wt% NSTO, the peak is at ∼60 K. After annealing in air, the *n-T* curve does not substantially change because the carrier density generated from oxygen vacancies of 1 h vacuum annealing is typically of the order of 10^{18} cm^{-3},[29] which is two orders of magnitude smaller than the carrier density from Nb doping for 0.5 wt% NSTO. However, the original peak at ∼60 K in the *M-T* curve disappears, accompanied by the disappearance of the ferromagnetic hysteresis loop. No similarity between the *n-T* and *M-T* curves for 0.05 and 0.1 wt% single crystals was observed [inset of Fig. 6(a)]. The similarity between the *n-T* and *M-T* curves in 0.5 wt% NSTO indicates that the ferromagnetism is sensitive to free carriers.

For as-received 0.05 and 0.1 wt% NSTO single crystals, no ferromagnetism was observed. The reason may be either the carrier density is not large enough or the initial concentration of oxygen vacancies is less. Since a higher concentration of Nb^{5+} ions can attract more O^{2-} and thus deform the crystal lattice, a larger doping could generate more deformation with oxygen vacancies in the lattice. Indeed, ferromagnetism was also seen in vacuum-annealed 0.05 wt% and 0.1 wt% NSTO single crystals.[20] Moreover, it was found that the saturation ferromagnetic moment of vacuum-annealed NSTO single crystals almost linearly scales with the doping level.[20] This further emphasizes the important role of carrier density in the ferromagnetism of NSTO.

Although both oxygen vacancies and Nb atoms can serve as donors of electrons for the Ti 3*d* orbitals in STO, they seem to be different. For example, there is no carrier freeze-out effect for NSTO even in the most lightly doped samples because the large dielectric constant of STO makes the activation energy of a hydrogenic-type donor quite small compared to the thermal energy at RT.[14] However, in reduced STO, the carrier freeze-out[30,31] can happen for the electrons originating from doubly charged donor centers—oxygen vacancies, i.e., the carrier density decreases dramatically with decreasing temperature. The donor level of oxygen vacancies is large, up to 80 meV separated from the conduction band of STO.[14] This reveals that the Ti 3*d* electrons originating from oxygen vacancies are naturally more inactive and localized.

As recently reported, localized Ti 3*d* electrons in STO can serve as magnetic centers to account for Kondo scattering[25] and ferromagnetism[32] in the $LaAlO_3/SrTiO_3$ system. Moreover, oxygen vacancies in the TiO_2 layer of STO can enhance the tendency for ferromagnetism considerably.[33] It seems that sufficient oxygen vacancies as well as carrier density are essential to produce this kind of indirect ferromagnetic exchange interaction. A possible mechanism for the ferromagnetism closely related to carrier density is the RKKY interaction.[34] Theoretically, the ferromagnetic RKKY interaction under the Weiss mean-field treatment can be strengthened by the increase of carrier density.[35,36] In the free-electron approximation, the RKKY exchange integral oscillates with the distance of magnetic ions at a period of $\lambda_F/2$ (see Refs. 37 and 38), where λ_F is the Fermi wavelength. The length scale $\lambda_F/2$ for 0.5 wt% NSTO single crystals is 1.93 nm[20] Considering a 0.5 wt% NSTO single crystal vacuum-annealed at 950 °C for 1 h, the diffusion length of oxygen vacancies is ∼6 μm and the distance among oxygen vacancies is estimated to be 2.53 nm,[20] which is comparable to the RKKY interaction length so that oxygen vacancies could interact with each other, mediated by the large number of free electrons from Nb doping. However, the indirect exchange coupling between impurity moments in semiconductors via the RKKY interaction is typically weak and yields ferromagnetism with a Curie temperature below room temperature.[39,40] In contrast, the Curie temperature in our system is high, and this needs further explanation. The normalized ferromagnetic moment for each Ti^{3+} center originating from oxygen vacancies is estimated to be ∼0.05 μ_B,[20] which is of the same order as the ferromagnetic moment of localized Ti 3*d* electron at the $LaAlO_3/SrTiO_3$ interface.[41] In addition, no signature of ferromagnetism was observed in the scanning SQUID study of NSTO films in Ref. 41, which is likely because the NSTO samples were annealed at 900 °C in the oxygen atmosphere to remove oxygen vacancies.[42]

In summary, we studied the electrical and magnetic properties of NSTO single crystals. Reversible RTFM was observed in highly doped (⩾0.5 wt%) NSTO single crystals and found to be induced by oxygen vacancies and closely related to free carriers. Ferromagnetic moments were found to mostly exist in the surface region of NSTO single crystals. Hysteretic MR as well as the important role of carrier density indicate the intrinsic signature of the ferromagnetism. The use of this kind of substrate to search for novel ferromagnetism in oxide thin films should be exercised with care due to the presence of ferromagnetism up to RT. Even though the ferromagnetism signal observed in the NSTO single crystals is weak, it is strong enough to interfere with magnetic signals of thin films grown on it.

*ariando@nus.edu.sg

[1]H. Ohno, Science **281**, 951 (1988).

[2]G. A. Prinz, Science **282**, 1660 (1998).

[3]T. Dietl, H. Ohno, F. Matsukura, J. Cibert, and D. Ferrand, Science **287**, 120109 (2000).

[4]Y. Matsumoto, M. Murakami, T. Shono, T. Hasegawa, T. Fukumura, M. Kawasaki, P. Ahmet, T. Chikyow, S. Koshihara, and H. Koinuma, Science **291**, 854 (2001).

[5]S. B. Ogale, R. J. Choudhary, J. P. Buban, S. E. Lofland, S. R. Shinde, S. N. Kale, V. N. Kulkarni, J. Higgins, C. Lanci, J. R.

Simpson, N. D. Browning, S. Das Sarma, H. D. Drew, R. L. Greene, and T. Venkatesan, Phys. Rev. Lett. **91**, 077205 (2003).

[6] J. He, S. F. Xu, Y. K. Yoo, Q. Z. Xue, H. C. Lee, S. F. Cheng, X. D. Xiang, and I. Takeuchi, Appl. Phys. Lett. **86**, 052503 (2005).

[7] M. Venkatesan, C. B. Fitzgerald, and J. M. D. Coey, Nature (London) **430**, 630 (2004).

[8] S. D. Yoon, Y. J. Chen, A. Yang, T. L. Goodrich, X. Zuo, D. A. Arena, K. Ziemer, C. Vittoria, and V. G. Harris, J. Phys.: Condens. Matter **18**, L355 (2006).

[9] N. H. Hong, J. Sakai, N. Poirot, and V. Brizé, Phys. Rev. B **73**, 132404 (2006).

[10] N. H. Hong, J. Sakai, and V. Brizé, J. Phys.: Condens. Matter **19**, 036219 (2007).

[11] S. Mal, S. Nori, C. Jin, J. Narayan, S. Nellutla, A. I. Smirnov, and J. T. Prater, J. Appl. Phys. **108**, 073510 (2010).

[12] N. H. Hong, N. Poirot, and J. Sakai, Phys. Rev. B **77**, 033205 (2008).

[13] K. van Benthem, C. Elsässer, and R. H. French, J. Appl. Phys. **90**, 6156 (2001).

[14] O. N. Tufter and P. W. Chapman, Phys. Rev. **155**, 796 (1967).

[15] G. Binnig, A. Baratoff, H. E. Hoenig, and J. G. Bednorz, Phys. Rev. Lett. **45**, 1352 (1980).

[16] F. Gervais, J. L. Servoin, A. Baratoff, J. G. Bednorz, and G. Binnig, Phys. Rev. B **47**, 8187 (1993).

[17] J. L. M. van Mechelen, D. van der Marel, C. Grimaldi, A. B. Kuzmenko, N. P. Armitage, N. Reyren, H. Hagemann, and I. I. Mazin, Phys. Rev. Lett. **100**, 226403 (2008).

[18] Z. Q. Liu, D. P. Leusink, W. M. Lu, X. Wang, X. P. Yang, K. Gopinadhan, Y. T. Lin, A. Annadi, Y. L. Zhao, A. R. Barman, S. Dhar, Y. P. Feng, H. B. Su, G. Xiong, T. Venkatesan, and Ariando, Phys. Rev. B **84**, 165106 (2011).

[19] D. P. Young, D. Hall, M. E. Torelli, Z. Fisk, J. L. Sarrao, J. D. Thompson, H.-R. Ott, S. B. Oseroff, R. G. Goodrich, and R. Zysler, Nature (London) **397**, 412 (1999).

[20] See Supplemental Material at, http://link.aps.org/supplemental/10.1103/PhysRevB.87.220405 for supporting data.

[21] "SIMS detection limits of selected elements in Si and SiO_2 under depth profiling conditions," Evans Analytical Group, 2007.

[22] M. L. Scullin, J. Ravichandran, C. Yu, M. Huijben, J. Seidel, A. Majumdar, and R. Ramesh, Acta Mater. **58**, 457 (2010).

[23] S. X. Zhang, S. B. Ogale, D. C. Kundaliya, L. F. Fu, N. D. Browning, S. Dhar, W. Ramadan, J. S. Higgins, R. L. Greene, and T. Venkatesan, Appl. Phys. Lett. **89**, 012501 (2006).

[24] Z. Q. Liu, Y. Ming, W. M. Lü, Z. Huang, X. Wang, B. M. Zhang, C. J. Li, K. Gopinadhan, S. W. Zeng, A. Annadi, Y. P. Feng, T. Venkatesan, and Ariando, Appl. Phys. Lett. **101**, 223105 (2012).

[25] A. Brinkman, M. Huijben, M. van Zalk, J. Huijben, U. Zeitler, J. C. Maan, W. G. van der Wiel, G. Rijnders, D. H. A. Blank, and H. Hilgenkamp, Nat. Mater. **6**, 493 (2007).

[26] A. D. Caviglia, S. Gariglio, C. Cancellieri, B. Sacepe, A. Fete, N. Reyren, M. Gabay, A. F. Morpurgo, and J.-M. Triscone, Phys. Rev. Lett. **105**, 236802 (2010).

[27] Ariando, X. Wang, G. Baskaran, Z. Q. Liu, J. Huijben, J. B. Yi, A. Annadi, A. Roy Barman, A. Rusydi, S. Dhar, Y. P. Feng, J. Ding, H. Hilgenkamp, and T. Venkatesan, Nat. Commun. **2**, 188 (2011).

[28] P. Moetakef, J. R. Williams, D. G. Ouellette, A. P. Kajdos, D. Goldhaber-Gordon, S. J. Allen, and S. Stemmer, Phys. Rev. X **2**, 021014 (2012).

[29] Z. Q. Liu, W. M. Lü, X. Wang, Z. Huang, A. Annadi, S. W. Zeng, T. Venkatesan, and Ariando, Phys. Rev. B **85**, 155114 (2012).

[30] Z. Q. Liu, D. P. Leusink, X. Wang, W. M. Lu, K. Gopinadhan, A. Annadi, Y. L. Zhao, X. H. Huang, S. W. Zeng, Z. Huang, A. Srivastava, S. Dhar, T. Venkatesan, and Ariando, Phys. Rev. Lett. **107**, 146802 (2011).

[31] Z. Q. Liu, C. J. Li, W. M. Lü, X. H. Huang, Z. Huang, S. W. Zeng, X. P. Qiu, L. S. Huang, A. Anndi, J. S. Chen, J. M. D. Coey, T. Venkatesan, and Ariando, Phys. Rev. X **3**, 021010 (2013).

[32] B. Kalisky, J. A. Bert, B. B. Klopfer, C. Bell, H. K. Sato, M. Hosoda, Y. Hikita, H. Y. Hwang, and K. A. Moler, Nat. Commun. **3**, 922 (2012).

[33] N. Pavlenko, T. Kopp, E. Y. Tsymbal, G. A. Sawatzky, and J. Mannhart, Phys. Rev. B **85**, 020407(R) (2012).

[34] M. A. Ruderman and C. Kittel, Phys. Rev. **96**, 99 (1954).

[35] T. Dietl, H. Ohno, and F. Matsukura, Phys. Rev. B **63**, 195205 (2001).

[36] S. Das Sarma, E. H. Hwang, and D. J. Priour, Jr., Phys. Rev. B **70**, 161203 (2004).

[37] J. M. D. Coey, M. Venkatesan, and C. B. Fitzgerald, Nat. Mater. **4**, 173 (2005).

[38] P. Bruno and C. Chappert, Phys. Rev. B **46**, 261 (1992).

[39] J. I. Inoue, Phys. Rev. B **67**, 125302 (2003).

[40] Y. J. Zhao, T. Shishidou, and A. J. Freeman, Phys. Rev. Lett. **90**, 047204 (2003).

[41] J. A. Bert, B. Kalisky, C. Bell, M. Kim, Y. Kikita, H. Y. Hwang, and K. A. Moler, Nat. Phys. **7**, 767 (2011).

[42] Y. Kozula, M. Kim, C. Bell, B. G. Kim, Y. Hikita, and H. Y. Hwang, Nature (London) **462**, 487 (2009).